

Attosecond Extreme Ultraviolet Vortices from High-Order Harmonic Generation

Carlos Hernández-García,^{1,3,*} Antonio Picón,² Julio San Román,¹ and Luis Plaja¹

¹*Grupo de Investigación en Óptica Extrema, Universidad de Salamanca, E-37008 Salamanca, Spain*

²*Argonne National Laboratory, Argonne, Illinois 60439, USA*

³*JILA and Department of Physics, University of Colorado at Boulder, Boulder, Colorado 80309-0440, USA*

(Received 27 March 2013; published 23 August 2013)

We present a theoretical study of high-order harmonic generation (HHG) and propagation driven by an infrared field carrying orbital angular momentum (OAM). Our calculations unveil the following relevant phenomena: extreme-ultraviolet harmonic vortices are generated and survive to the propagation effects, vortices transport high-OAM multiples of the corresponding OAM of the driving field and, finally, the different harmonic vortices are emitted with similar divergence. We also show the possibility of combining OAM and HHG phase locking to produce attosecond pulses with helical pulse structure.

DOI: [10.1103/PhysRevLett.111.083602](https://doi.org/10.1103/PhysRevLett.111.083602)

PACS numbers: 42.50.Tx, 32.30.Rj, 42.65.Ky

Helical phased beams, also called optical vortices, are structures of the electromagnetic field with a spiral phase ramp about a point-phase singularity. The phase wind imprints an orbital angular momentum (OAM) to the beam, in addition to the intrinsic angular momentum associated with the polarization [1–3]. As light-matter interaction is inherently connected with the exchange of momentum, OAM can also be transferred to atoms [4–6], molecules [7,8], or an ensemble of atoms [9–13]. Optical vortices have potential technological applications in optical communication [14,15], micromanipulation [16], phase-contrast microscopy [17,18], and others [19]. In recent years an interest has burgeoned in imprinting phase singularities in the extreme ultraviolet-x-ray light generated both in synchrotron and x-ray free-electron laser facilities [20–22]. In this short-wavelength regime one can drastically reduce the diffraction limit, as well as exploit the selectively site-specific excitation, with important impacts in microscopy [23,24] and spectroscopy [25].

Nonlinear optics has been demonstrated to be a very useful physical process to manipulate the OAM of a beam. For instance, it has been used to increase the OAM beam charge in ring monolithic cavities [26]. Another high nonlinear process, such as high-order harmonic generation (HHG) [27], has been recently used by Zürich and co-workers to imprint phase singularities to shorter-wavelength light, producing vortices in the extreme ultraviolet (XUV) [28]. The HHG process, which occurs during the interaction of intense lasers with matter, can be understood with simple semiclassical arguments, where energetic photons are generated during the rescattering of ionized electrons with their parent ion [29,30]. As a result, the non-perturbative harmonic spectrum extends towards the XUV forming a *plateau* of harmonics with similar intensities. The interference of the radiation emitted from different atoms in the target, known as phase matching, plays a relevant role in the propagation of HHG in macroscopic media [31].

The confluence of OAM and HHG constitutes an extraordinarily promising perspective. For instance, the phase

twist is not imprinted directly to the short-wavelength radiation, but to the fundamental field. Therefore, it requires a single setup (diffractive mask, for instance) to imprint OAM to the fundamental field [32,33], that will be subsequently transferred to the rainbow of harmonic wavelengths by nonlinear conversion. On the other hand, high-order harmonics have extraordinary temporal coherence qualities [34], a unique feature that has triggered a revolutionary metrology tool for the temporal characterization of ultrafast processes at the atomic scale (both spatially and temporally) [35,36]. Two decades ago, it was demonstrated that the higher part of the HHG spectra can be used to synthesize short XUV pulses of attosecond duration [37–40]. It is, therefore, an appealing possibility if such attosecond pulses can be synthesized with OAM. In addition, the new HHG generation schemes, based on the present development of midinfrared (mid-IR) laser sources, show that keV x-ray radiation can be obtained from the HHG process in a tabletop system [41], as well as that the zeptosecond era could be closer than expected [42]. Therefore, there is no fundamental obstacle for upshifting the XUV OAM beams to extremely short temporal structures, or to generate them in the soft x-ray regime.

A surprising finding of the recent HHG-OAM experiment [28] is that the topological charge of the harmonic vortices is nearly equal to 1, i.e., that of the fundamental field. This is counterintuitive in terms of the present understanding of HHG with intense fields, in which the phase of the harmonics scales roughly with the harmonic order. Zürich and co-workers attribute the appearance of only low-charged vortices to parametric instabilities in the nonlinear propagation of the fundamental field. The theoretical treatment of HHG and propagation in the nonlinear regime presented in the experiment is extremely challenging. Nevertheless, at present, it is recognized that a detailed theoretical treatment including propagation effects is needed, even in the linear regime, to elucidate some of the fundamental aspects of the HHG OAM conversion

[43]. For instance, it is presently uncertain that high-charge vortices might be obtained even if no parametric instabilities are present, as they would have to survive phase-matching effects during propagation. Finally, it is also an open question whether attosecond HHG OAM pulses can be generated and be resilient to propagation as well.

In this Letter we present a pioneering theoretical study of the HHG process from an IR field carrying OAM of topological charge ℓ , in an intensity-pressure regime where the nonlinear propagation instabilities, which lead to the observation of low-charged vortices in [28], can be neglected. For the same reason, in this linear propagation regime, one should not expect strong effects due to imperfections in the vortex (e.g., phase noise or astigmatism). We prove that (i) XUV harmonics vortices are generated and survive to the propagation effects, (ii) each harmonic has a topological charge of $q\ell$, q being the harmonic order, (iii) all the harmonics are emitted with similar divergence and, (iv) attosecond pulses carrying OAM can be generated and also survive propagation.

We compute harmonic propagation using the electromagnetic field propagator [44]. We discretize the target (gas cell or gas jet) into elementary radiators (sketched in Fig. 1), and propagate the emitted field $E_j(r, t)$ to the detector,

$$\mathbf{E}_j(\mathbf{r}_d, t) = \frac{q_j \mathbf{s}_d}{c^2 |\mathbf{r}_d - \mathbf{r}_j|} \left[\mathbf{s}_d \times \mathbf{a}_j \left(t - \frac{|\mathbf{r}_d - \mathbf{r}_j|}{c} \right) \right], \quad (1)$$

where q_j is the charge of the electron, \mathbf{s}_d is the unitary vector pointing to the detector, and \mathbf{r}_d and \mathbf{r}_j are the position vectors of the detector and of the elementary radiator j , respectively. The dipole acceleration \mathbf{a}_j of each elementary source is computed using the SFA+ method, an extension of the standard strong field approach with good quantitative accuracy [45]. Note that Eq. (1) assumes the harmonic radiation to propagate with the vacuum phase velocity, which is a reasonable assumption for high-order harmonics. Finally, the total field at the detector is computed as the coherent addition of the elementary contributions. Propagation effects in the fundamental field such as the free charges and neutrals, as well as absorption in the propagation of the harmonics, are

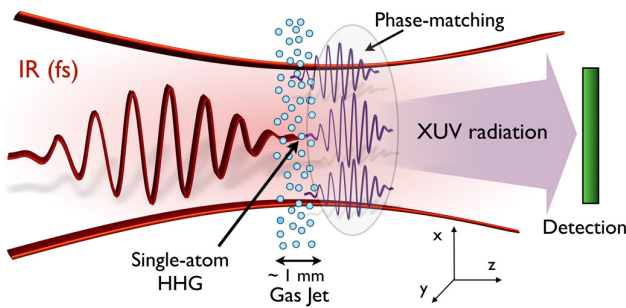


FIG. 1 (color online). Schematic view of a HHG experiment: an intense fs IR field is focused into a gas jet. Each atom interacting with the IR field emits XUV radiation. The harmonic signal at the detector is strongly affected by the phase matching of the radiation from the emitters.

also taken into account. One of the advantages of this method is that it is well fitted to compute high-order harmonic propagation in nonsymmetric geometries; therefore, it is specially suited for computing HHG driven by beams carrying OAM. The method has been successfully used for describing regular HHG with near- and mid-IR lasers, in good agreement with experiments [41,46]. More information on this method and the SFA+ may be found in Refs. [47,48].

In order to implement the OAM beams, we consider the Laguerre-Gaussian (LG) modes in the paraxial approximation [1]; i.e., the beam propagates in a well-defined direction (in our case the z axis) as a plane wave modulated by the slowly varying transverse amplitude (written in cylindrical coordinates)

$$LG_{\ell,p}(\rho, \phi, z) = E_0 \frac{W_0}{W(z)} \left(\frac{\rho}{W(z)} \right)^{|\ell|} L_p^{|\ell|} \left[\frac{2\rho^2}{W^2(z)} \right] \exp\left(-\frac{\rho^2}{W^2(z)}\right) \times \exp\left(ik\frac{\rho^2}{2R(z)} + i\zeta(z) + i\ell\phi\right). \quad (2)$$

$W(z) = W_0 \sqrt{1 + (z/z_0)^2}$ is the beam width, where W_0 is the beam waist, $W_0 = \sqrt{\lambda z_0/\pi}$ (z_0 being the Rayleigh length); $R(z)$ is the wave front radius of curvature, given by $R(z) = z[1 + (z_0/z)^2]$; $\zeta(z)$ is the Gouy phase, which is given by $\zeta(z) = -(|\ell| + 2p + 1)\tan^{-1}(z/z_0)$; k is the wave number; and, $L_p^{|\ell|}[x]$ are the associated Laguerre polynomials. The indices $\ell = 0, \pm 1, \pm 2, \dots$ and $p = 0, 1, 2, \dots$ correspond to the topological charge and the number of radial nodes of the mode, respectively.

We consider as a fundamental field a beam carrying OAM with $\ell = 1$, or $\ell = 2$, and $p = 0$, with a beam waist of $W_0 = 30 \mu\text{m}$, and, hence, a Rayleigh range $z_0 = 3.5 \text{ mm}$. The amplitude of the field, E_0 is chosen to give a peak intensity at focus of $1.4 \times 10^{14} \text{ W/cm}^2$. The laser pulse is assumed to be a \sin^2 envelope of 5.8 cycles (15.4 fs) FWHM and 800 nm wavelength. In Figs. 2(a) and 2(b) we present the intensity and phase profiles of the $LG_{1,0}$ mode at the focus position for the above parameters. As it can be observed in plot (b), the term $e^{i\phi}$ imprints an azimuthal phase variation on the beam from $-\pi$ to π .

In our simulations, the OAM beam is focused into an argon gas jet, which is directed along the x axis, and modeled by a Gaussian distribution along the y and z dimensions (whose FWHM is $500 \mu\text{m}$), and a constant profile along its axial dimension, x (see Fig. 1), with a peak density of $10^{17} \text{ atoms/cm}^3$. Under these conditions, the two main contributions for phase matching are the intrinsic phase of the harmonics (i.e., the phase acquired in their generation) and the Gouy phase. Fortunately, these two contributions tend to compensate if the gas jet is placed after the focus position, resulting in optimal longitudinal phase-matching conditions [49,50]. For that reason, we place the gas jet 2 mm after the focus position. In addition, as mentioned above, the pulse intensity and the gas density are chosen such that the nonlinear effects of the

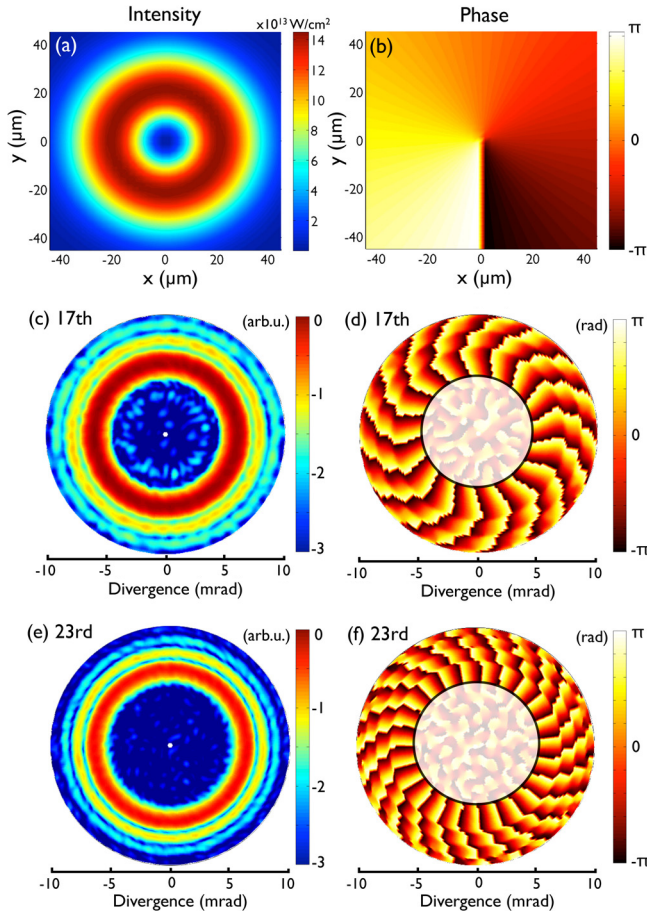


FIG. 2 (color online). (a) Intensity and (b) phase transversal profiles of the $LG_{1,0}$ mode of the fundamental beam at the focus position, with a beam waist of $W_0 = 30 \mu\text{m}$. The amplitude E_0 in Eq. (2), is chosen to give a peak intensity of $1.4 \times 10^{14} \text{ W/cm}^2$ at the focus. (c,e) Intensity and (d,f) phase angular profiles for the 17th-23rd harmonics. Note that the intensity profiles are given in logarithmic scale. The resulting topological charge can be obtained from (d) and (f) resulting in $\ell = 17$ for the 17th and $\ell = 23$ for the 23rd harmonic.

propagation can be neglected both for the IR as well as the XUV fields.

In Figs. 2(c)–2(f) we present the intensity-phase angular profiles of the 17th (c),(d) and 23rd (e),(f) harmonics generated with the $LG_{1,0}$ mode. Two main conclusions arise from these plots. First, the radius of the annular intensity distribution is similar for the two selected harmonics; thus, they are emitted with similar divergence. In fact, similar divergence emission can be observed for the whole harmonic spectra; see Fig. 3(a). Second, the phase plots show that the charge of the q th-order harmonic is q , which, as mentioned above, is expected from the HHG theory [43]. The harmonics generated with the $LG_{2,0}$ mode (not shown) fulfill also these properties, appearing with a similar divergence angle and the q th-harmonic having $2q$ topological charge.

Figure 3(a) shows the angular profile of the spectrum diverging along the y axis (transverse to propagation) for

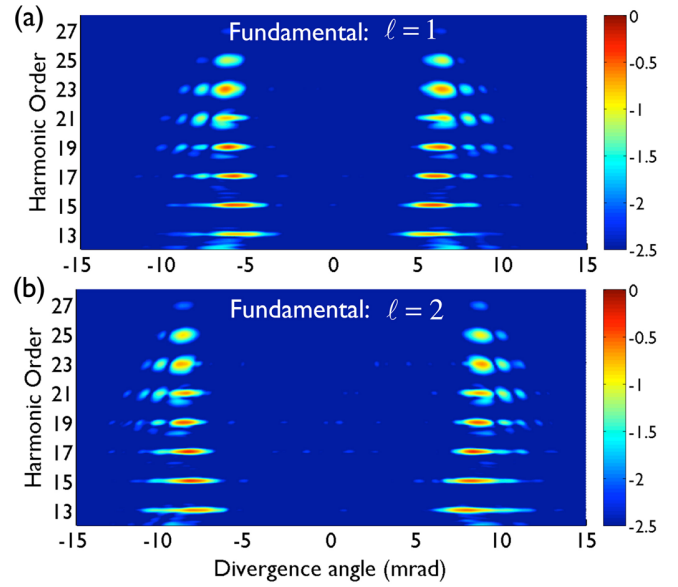


FIG. 3 (color online). Angular distribution of the harmonic spectra generated by an optical vortex of charge (a) $\ell = 1$ ($LG_{1,0}$) and (b) $\ell = 2$ ($LG_{2,0}$). The parameters for plot (a) are the same as in Fig. 2, whereas for plot (b) we have changed the topological charge, $\ell = 2$, and the amplitude E_0 in Eq. (2) has been increased to give a peak intensity at the focus of $1.4 \times 10^{14} \text{ W/cm}^2$. The radii of the generated XUV vortex is similar for all the harmonics, being longer for the higher topological charge. The spectra are presented assuming a Al filter plate of 500 nm in thickness.

the same parameters as in Fig. 2. We can observe that the harmonics in the plateau region exhibit a double-fringe profile corresponding to the vortex intensity distribution, whose radius is similar for all the harmonics, a feature that was also observed in [28]. For a fundamental beam of topological charge $\ell = 2$, in particular a $LG_{2,0}$ mode, we also observe that the high harmonics are emitted as XUV vortices with similar radii, see Fig. 3(b), being the radii longer than those obtained with $\ell = 1$. Therefore, HHG leads to a perfect vortex generation process in terms of its applicability [51], as all these XUV vortices of topological charge $q\ell$ are emitted with similar size.

Let us now look at how the XUV vortices are emitted temporally. One of the most exciting perspectives of HHG by intense lasers is the possibility of synthesizing XUV pulses of sub-femtosecond duration [37]. An attosecond pulse train is obtained by selecting the higher frequencies of the harmonic spectrum near the cut-off [39]. For the correct synthesis, the spectrum should approximately satisfy the two following conditions: on one side its structure should approach to that of a frequency comb, in which the harmonic intensities are similar; on the other side, the relative phase between the harmonics should be nearly constant (phase locking) [37]. These two conditions are well satisfied in the typical harmonic spectrum generated during the interaction of an intense field with an atom. Fortunately, HHG driven by OAM beams leads to the generation of XUV

OAM beams with similar divergence, therefore allowing for the synthesis of an helical attosecond pulse train.

In Fig. 4(a) we present the temporal evolution of the high-harmonic signal shown in Figs. 2 and 3(a). As the fundamental laser pulse consists of many cycles, 5.8 cycles (15.4 fs), a helical attosecond pulse train is obtained, i.e., an attosecond pulse train delayed along the azimuthal coordinate according to the phase variation of the fundamental $LG_{1,0}$ beam. Note that the time separation at a fixed angle between the pulses of the helical structure is half the period of the driving field (1.33 fs). On the right side of Fig. 4(a) we show the attosecond pulse train obtained at different azimuthal angles ϕ . Note that although each high-harmonic OAM beam is generated with $\ell = q$, as we select many harmonic orders (see Fig. 3), the pulse train structure remains similar.

It is also possible to obtain an isolated attosecond pulse using few-cycle driving pulses [38,40], since high-order harmonics are then generated in a single rescattering event. We show in Fig. 4(b) the temporal structure of the XUV OAM beam driven by a few-cycle pulse, 1.4 cycles (3.8 fs). The OAM imprints a different carrier-envelope phase in

the fundamental pulse over the azimuthal angle ϕ , and thus, the helical attosecond structure varies from an isolated attosecond pulse, generated around $\phi = 60^\circ$, to a double pulse structure, around $\phi = 120^\circ$. As a consequence, we obtain in a single shot the map of all the attosecond pulse structures for different carrier-envelope phase values. We believe that these helical attosecond structures, obtained in a single shot, are a powerful tool for pump-probe experiments with attosecond resolution.

In conclusion, we have demonstrated the obtaining of high-harmonic XUV vortices with topological charge $q\ell$ (q being the harmonic order) from HHG driven by an IR beam carrying OAM with topological charge ℓ . We have shown that all the harmonics are emitted with similar divergence, and that these structures are robust under the effects of phase matching during propagation. We have also proven that the highest order harmonics can be used to synthesize OAM attosecond pulses, that exhibit an attosecond helical structure. We believe that the combination of the properties of optical vortices carrying OAM with the spatiotemporal characteristics of high-order harmonic

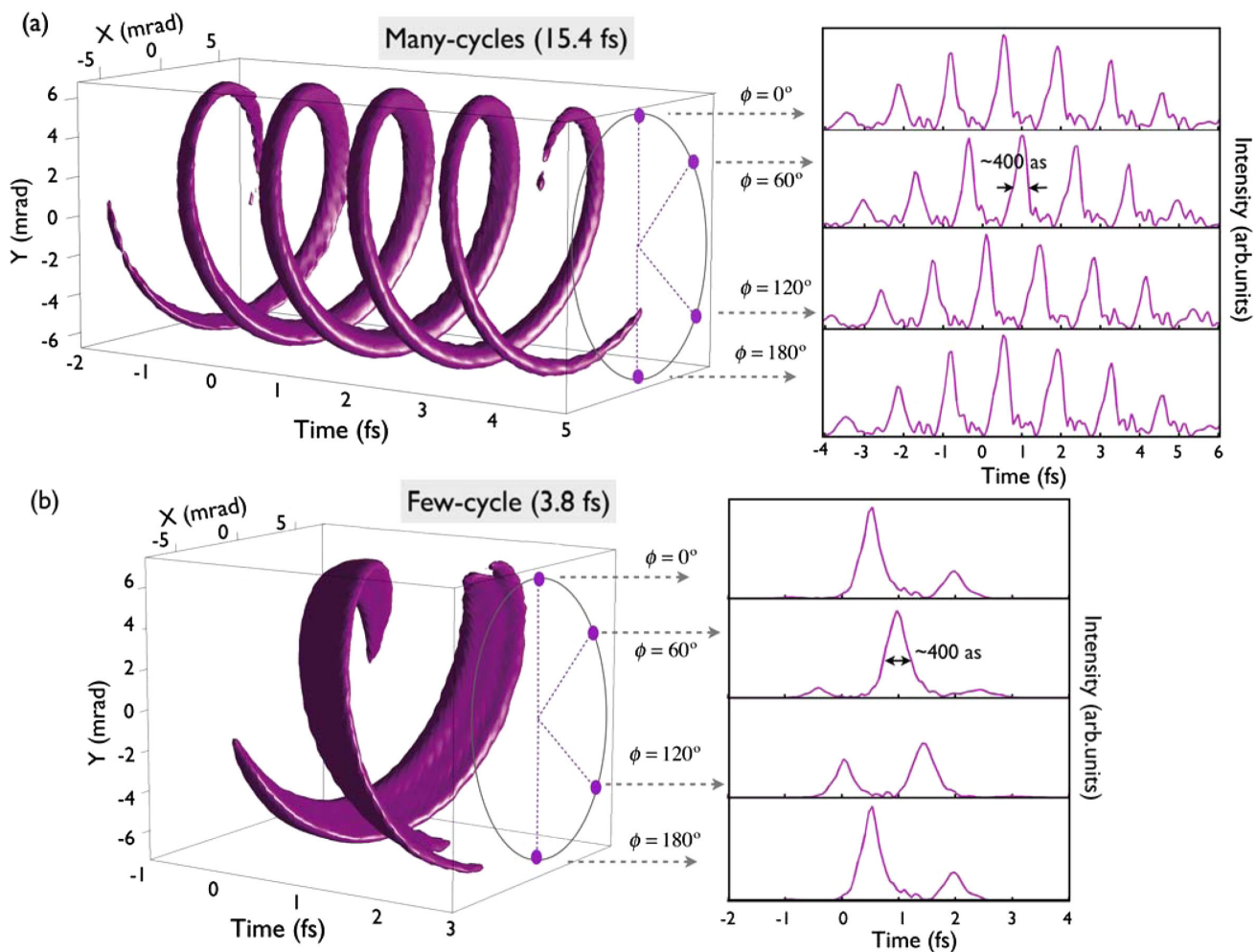


FIG. 4 (color online). Temporal evolution of the high-harmonic signal driven by (a) a multicycle pulse—5.8 cycles (15.4 fs) FWHM—and (b) a few-cycle pulse—1.4 cycles (3.8 fs) FWHM. The XUV OAM is emitted in the form of an helical attosecond structure, whose detailed form is presented on the right side for different azimuthal angles ϕ : 0° , 60° , 120° , and 180° .

generation and propagation opens a new and promising perspective in ultrafast science.

We acknowledge I. J. Sola for valuable discussions, and support from Spanish MINECO (FIS2009-09522) and Centro de Láseres Pulsados (CLPU). C. H.-G. acknowledges support by a Marie Curie International Outgoing Fellowship within the EU Seventh Framework Programme for Research and Technological Development (2007–2013), under REA grant Agreement No. 328334. A. P. acknowledges fruitful discussions with I. McNulty and S. H. Southworth, and the financial support of the U.S. Department of Energy, Basic Energy Sciences, Office of Science, under Contract No. DE-AC02-06CH11357.

*carloshergar@usal.es

- [1] L. Allen, M. W. Beijersbergen, R. J. C. Spreeuw, and J. P. Woerdman, *Phys. Rev. A* **45**, 8185 (1992).
- [2] G. F. Calvo, A. Picón, and E. Bagan, *Phys. Rev. A* **73**, 013805 (2006).
- [3] M. S. Soskin and M. V. Vasnetsov, *Prog. Opt.* **42**, 219 (2001).
- [4] A. Picón, A. Benseny, J. Mompert, J. R. Vázquez de Aldana, L. Plaja, G. F. Calvo, and L. Roso, *New J. Phys.* **12**, 083053 (2010).
- [5] R. Jáuregui, *Phys. Rev. A* **70**, 033415 (2004).
- [6] M. Babiker, W. L. Power, and L. Allen, *Phys. Rev. Lett.* **73**, 1239 (1994).
- [7] A. Alexandrescu, D. Cojoc, and E. Di Fabrizio, *Phys. Rev. Lett.* **96**, 243001 (2006).
- [8] M. Babiker, C. R. Bennett, D. L. Andrews, and L. C. D. Romero, *Phys. Rev. Lett.* **89**, 143601 (2002).
- [9] J. W. R. Tabosa and D. V. Petrov, *Phys. Rev. Lett.* **83**, 4967 (1999).
- [10] R. Inoue, N. Kanai, T. Yonehara, Y. Miyamoto, M. Koashi, and M. Kozuma, *Phys. Rev. A* **74**, 053809 (2006).
- [11] S. J. van Enk, *Quantum Opt.* **6**, 445 (1994).
- [12] K. T. Kapale and J. P. Dowling, *Phys. Rev. Lett.* **95**, 173601 (2005).
- [13] M. F. Andersen, C. Ryu, P. Cladé, V. Natarajan, A. Vaziri, K. Helmerson, and W. D. Phillips, *Phys. Rev. Lett.* **97**, 170406 (2006).
- [14] J. Wang *et al.*, *Nat. Photonics* **6**, 488 (2012).
- [15] X. Cai, J. Wang, M. J. Strain, B. Johnson-Morris, J. Zhu, M. Sorel, J. L. O'Brien, M. G. Thompson, and S. Yu, *Science* **338**, 363 (2012).
- [16] D. G. Grier, *Nature (London)* **424**, 810 (2003).
- [17] S. Fürhapter, A. Jesacher, S. Bernet, and M. Ritsch-Marte, *Opt. Lett.* **30**, 1953 (2005).
- [18] A. Jesacher, S. Fürhapter, S. Bernet, and M. Ritsch-Marte, *Phys. Rev. Lett.* **94**, 233902 (2005).
- [19] *Twisted Photons*, edited by J. P. Torres and L. Torner (Wiley-VCH, Weinheim, 2011).
- [20] A. G. Peele, P. J. McMahon, D. Paterson, C. Q. Tran, A. P. Mancuso, K. A. Nugent, J. P. Hayes, E. Harvey, B. Lai, and I. McNulty, *Opt. Lett.* **27**, 1752 (2002).
- [21] S. Sasaki and I. McNulty, *Phys. Rev. Lett.* **100**, 124801 (2008).
- [22] E. Hemsing, A. Marinelli, and J. B. Rosenzweig, *Phys. Rev. Lett.* **106**, 164803 (2011).
- [23] A. Sakdinawat and Y. Liu, *Opt. Lett.* **32**, 2635 (2007).
- [24] K. A. Nugent, *Adv. Phys.* **59**, 1 (2010).
- [25] M. van Veenendaal and I. McNulty, *Phys. Rev. Lett.* **98**, 157401 (2007).
- [26] A. B. Matsko, A. A. Savchenkov, D. Strekalov, and L. Maleki, *Phys. Rev. Lett.* **95**, 143904 (2005).
- [27] X. F. Li, A. L'Huillier, M. Ferray, L. A. Lompré, and G. Mainfray, *Phys. Rev. A* **39**, 5751 (1989).
- [28] M. Zürch, C. Kern, P. Hansinger, A. Dreischuh, and Ch. Spielmann, *Nat. Phys.* **8**, 743 (2012).
- [29] K. J. Schafer, B. Yang, L. F. DiMauro, and K. C. Kulander, *Phys. Rev. Lett.* **70**, 1599 (1993).
- [30] P. B. Corkum, *Phys. Rev. Lett.* **71**, 1994 (1993).
- [31] T. Popmintchev, M. Chen, P. Arpin, M. M. Murnane, and H. C. Kapteyn, *Nat. Photonics* **4**, 822 (2010).
- [32] I. J. Sola, V. Collados, L. Plaja, C. Méndez, J. S. Román, C. Ruiz, I. Arias, A. Villamarín, J. Atencia, M. Quintanilla, and L. Roso, *Appl. Phys. B* **91**, 115 (2008).
- [33] K. Yamane, Y. Toda, and R. Morita, *Opt. Express* **20**, 18986 (2012).
- [34] F. Krausz and M. Ivanov, *Rev. Mod. Phys.* **81**, 163 (2009).
- [35] P. Salières, A. Maquet, S. Haessler, J. Caillat, and R. Taieb, *Rep. Prog. Phys.* **75**, 062401 (2012).
- [36] P. B. Corkum and F. Krausz, *Nat. Phys.* **3**, 381 (2007).
- [37] G. Farkas and C. Toth, *Phys. Lett. A* **168**, 447 (1992).
- [38] I. P. Christov, M. M. Murnane, and H. C. Kapteyn, *Phys. Rev. Lett.* **78**, 1251 (1997).
- [39] P. M. Paul, E. S. Toma, P. Breger, G. Mullot, F. Augé, Ph. Balcou, H. G. Muller and P. Agostini, *Science* **292**, 1689 (2001).
- [40] M. Hentschel, R. Kienberger, C. Spielmann, G. A. Reider, N. Milosevic, U. Heinzmann, M. Drescher, and F. Krausz, *Nature (London)* **414**, 509 (2001).
- [41] T. Popmintchev, M.-C. Chen, D. Popmintchev, P. Arpin, S. Brown, S. Alisauskas, G. Andriukaitas, T. Balciunas, O. Mücke, A. Pugzlys, A. Baltuska, B. Shim, S. E. Schrauth, A. Gaeta, C. Hernández-García, L. Plaja, A. Becker, A. Jaroń-Becker, M. M. Murnane, and H. C. Kapteyn, *Science* **336**, 1287 (2012).
- [42] C. Hernández-García, J. A. Pérez-Hernández, T. Popmintchev, M. M. Murnane, H. C. Kapteyn, A. Jaroń-Becker, A. Becker, and L. Plaja, *Phys. Rev. Lett.* **111**, 033002 (2013).
- [43] S. Patchkovskii and M. Spanner, *Nat. Phys.* **8**, 707 (2012).
- [44] C. Hernández-García, J. A. Pérez-Hernández, J. Ramos, E. C. Jarque, L. Roso, and L. Plaja, *Phys. Rev. A* **82**, 033432 (2010).
- [45] J. A. Pérez-Hernández, L. Roso, and L. Plaja, *Opt. Express* **17**, 9891 (2009).
- [46] C. Hernández-García, I. J. Sola, and L. Plaja, *Phys. Rev. A* (to be published).
- [47] J. A. Pérez-Hernández, C. Hernández-García, J. Ramos, E. Conejero Jarque, L. Plaja, and L. Roso, *New Methods For Computing High-Order Harmonic Generation and Propagation*, Springer Series in Chemical Physics Vol. 100 (Springer, New York, 2011), Chap. 7, p. 145.
- [48] C. Hernández-García and L. Plaja, *J. Phys. B* **45**, 074021 (2012).
- [49] P. Salières, A. L'Huillier, and M. Lewenstein, *Phys. Rev. Lett.* **74**, 3776 (1995).
- [50] P. Balcou, P. Salières, A. L'Huillier, and M. Lewenstein, *Phys. Rev. A* **55**, 3204 (1997).
- [51] A. S. Ostrovsky, C. Rickenstorff-Parrao, and V. Arrizón, *Opt. Lett.* **38**, 534 (2013).